Photoacoustic and ultrasonic coimage with a linear transducer array

Yaguang Zeng, Da Xing, Yi Wang, Bangzhen Yin, and Qun Chen

Institute of Laser Life Science, South China Normal University, Guangzhou 510631, China

Received April 2, 2004

A technique is developed to simultaneously acquire ultrasound and photoacoustic (PA) images based on a linear transducer array. The system uses conventional ultrasound for rapid identification of potential targets. After a target is identified, the ultrasound echo and PA signals can be simultaneously obtained with optimized excitation and a signal collection sequence. The corresponding ultrasound impedance and optical absorption images are reconstructed with a phase-controlled algorithm. The approach can effectively reduce the artifacts associated with a conventional filter backprojection algorithm used in PA imaging by linear scanning. The technique provides a new approach for practical applications. © 2004 Optical Society of America

OCIS codes: 170.5120, 170.3010, 170.7180.

In the past decade, detailed studies describing photoacoustic (PA) tomography have been presented.[1–6] PA tomography combines the merits of both pure ultrasound and optical imaging. It can produce high-resolution and high-contrast tissue imaging. However, there are many factors that require careful consideration before PA tomography can be used for practical medical diagnosis. To minimize the absorption and scattering during the propagation of the incident laser beam, the location of the entry port of the light beam should be chosen to be as close as possible to the potential target. Practical applications require fast data acquisition. This can be accomplished only by use of a detector array rather than a single detector. PA image reconstruction with a transducer array was reported recently.[7,8] In Ref. 7 the PA signals were acquired by rotating samples. In Ref. 8 the PA signals were acquired by use of an arc transducer array with a limited viewing angle without moving either the sample or the transducer array. For clinical applications the latter is obviously more practical. That study applied a filter backprojection algorithm to reconstruct the optical absorption distribution.[8] That method has a severe disadvantage: Artificial signals resulting from backprojection from non-PA sources can cause distortion in reconstructed images. Thus an improved system design and reconstruction algorithm are required.

In this Letter we demonstrate a prototype instrument that can simultaneously acquire ultrasound and PA images. A linear transducer array is used as a conventional ultrasound generator and detector and as a PA detector simultaneously. After a potential target is identified with the conventional ultrasound imaging, the corresponding PA image and ultrasound image are acquired simultaneously. The PA signal collection and processing are similar to those used for conventional ultrasound imaging. The transducer clusters are dynamically selected to perform linear scanning. Signals from each dynamically selected cluster are processed by the phase-controlled circuit of the system for optimal directionality and spatial focus. By use of the phase-controlled circuit, PA signals can be detected from only a focused region. The technique thus eliminates artifacts when a backprojection algorithm is used in linear scanning.

The hardware setup is based on a modified B-mode system (Model EUB-240, Hitachi, Japan) with a linear transducer array of 320 elements (0.1 mm × 8 mm). The linear array and phantoms were both immersed in water for better coupling of acoustic waves.[9] With a clock frequency of 4 kHz a conventional ultrasound image can be obtained for quick screening of a target. The secondary clock frequency of 30 Hz is used to trigger the YAG laser (MOPO, Spectrum Physics, 532 nm, pulse mode of 30 Hz with 7-ns width) for PA excitation and to synchronize the transducer clusters for detection of ultrasound echoes and PA signals. The data acquisition involves a sequence of ultrasound and PA events that can be summarized as follows: A dynamic cluster with 44 elements and an oscilloscope (TDS3032, Tektronix) are triggered by the clock signal at the same time. The active cluster generates a 70-ns focal pulse ultrasound. The Q-switched YAG laser is triggered after a 165-μs delay time to avoid overlap between the ultrasound echo and the PA signals. The laser beam is homogenized with a ground glass and introduced into the target to generate PA signals. The active cluster of line arrays serves as a cluster detector and receives the ultrasound echo and the PA signals successively. The signals are transferred to a personal computer for image reconstruction.

Ultrasound echoes and PA signals are acquired by a phase-controlled focusing technique that has the following advantages: First, as in conventional ultrasound imaging, the ultrasound sent to and the echoes detected from a particular target location are maximized (focused). More important, for our application, PA signals collected by the active cluster of transducers are also focused. That is, with the phase-controlled circuit, PA signals from a particular location along the central axis of the cluster of transducers are made coherent, whereas the PA signals from other locations tend to cancel each other because of the difference in their phases.

0146-9592/04/151760-03$15.00/0

The relationship between a PA signal and the distribution of optical absorption can be expressed as[10]

$$\oint\!\!\!\oint_{|r'-r_i|v_0 t} A(r')\mathrm{d}r' = \frac{4\pi c_p}{\beta I_0 v_0 \tau_0}\, t \int_0^t p(r,\tau)\mathrm{d}\tau\,, \qquad (1)$$

where $A(r')$ is the fractional energy absorption per unit volume of soft tissue, $p(r,\tau)$ is the PA pressure, β is the isobaric volume expansion coefficient, c_p is the specific heat, τ_0 is the pulse laser width, and v_0 is the sound velocity in the target, respectively. In practice, $p(r,\tau)$ cannot be measured directly because the impulse response of the detector is not a delta function. We compute $p(r,\tau)$ as[7]

$$p(r,\tau) = \mathrm{IFFT}\left[\frac{p'(r,\omega)}{I(\omega)}\right]\left\{\frac{1}{2}\left[1+\cos\left(\frac{\pi\omega}{\omega_0}\right)\right]\right\}, \qquad (2)$$

where $I(\omega)$ and $p'(r,\omega)$ are the Fourier transform of the impulse signal of the detector and the PA recorded by the detector, respectively. The impulse response of the detector was measured by illuminating its front surface with a weak laser pulse.[7] The aphorizing function $[1+\cos(\pi\omega/\omega_0)]/2$ was used to bandwidth limit the signal to ω_0. In our experiment we processed all our data with a cutoff frequency of $\omega_0 = 5$ MHz.

Two numerically simulated cylinders were reconstructed with both filter backprojection and phase-controlled algorithms based on linear scanning. PA pressures were calculated with the mathematical expressions.[11] For the simulations we assumed a linear array with 400 elements for use in signal detection. For the filter backprojection, each transducer collects signals independently. For the phase-controlled algorithm, each dynamic cluster consists of 50 transducers (a total of 350 sampling points). Figure 1(a) shows the physical locations of the sound sources used for the simulation. PA signals are generated only at the highlighted locations in the figure. An image reconstructed based on the filter backprojection algorithm is shown in Fig. 1(b); the detector array is aligned in the horizontal axis of Fig. 1(a). Figure 1(c) is the image reconstructed based on the phase-controlled algorithm. Comparing Figs. 1(b) and 1(c), the image reconstructed based on the filter backprojection algorithm has severe artifacts. The nature of the artifacts matches well with that observed experimentally.[8]

The theoretical prediction and the actual physical installation were tested experimentally. To simulate the optical properties of tissue, a cylindrical turbid phantom with a 3.1-cm diameter was made with water (100 ml), agar (3 g), and Intralipid (5 ml, 20%).[12] Effective attenuation coefficient μ_{eff} of the phantom cylinder was 1.2 cm^{-1}, similar to that of normal breast tissue *in vivo*. To simulate tumors in normal tissue, two spherical target absorbers of 3.5 mm in diameter were embedded 5 mm below the surface of the cylindrical phantom. The spheres were made of the same optically turbid agar mixed with Trypan Blue (0.005 g, $\mu_a = 0.5\ \mathrm{cm}^{-1}$). The distance between the spheres was ~10 mm.

Figure 2 shows typical ultrasound and PA signals collected by one cluster. Each data point is a result of averaging 100 signals. In Fig. 2 signals A, B, and C are the ultrasound echoes from the phantom surface, the embedded absorber, and the bottom of the phantom, respectively. The YAG laser was triggered with a 165-μs delay after the cluster and the oscilloscope were triggered. Signal D, at 165 μs, is due to the sound pressure generated at the transducer surface by scattered light. When the laser pulse reached the embedded light absorber, a PA signal was generated. The time for the PA signal to reach the transducers was determined by the sound speed inside the sample and the distance between the absorber and the corresponding detector. The PA signal is shown as signal E in Fig. 2.

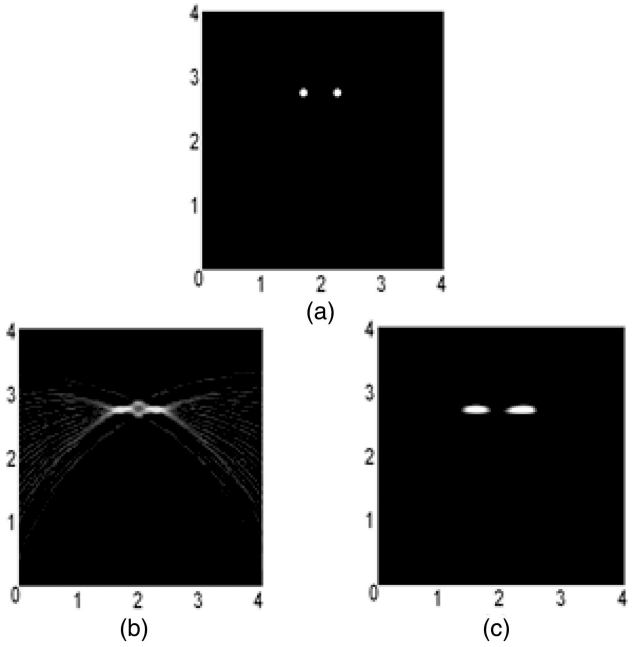

Fig. 1. (a) Physical locations of numerical simulation sound sources, (b) image reconstructed by the filter backprojection algorithm, (c) image reconstructed by the phase-controlled focusing algorithm.

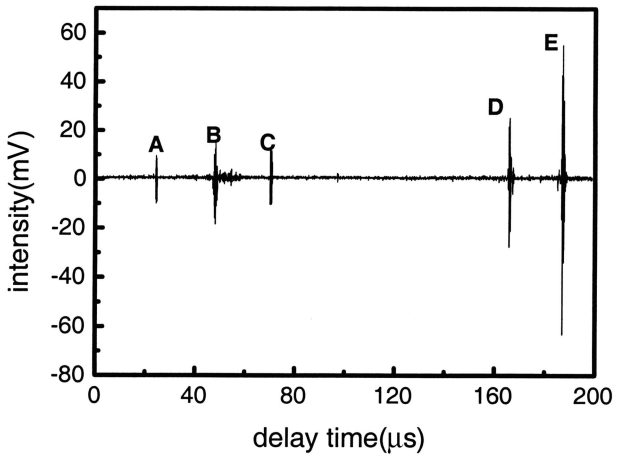

Fig. 2. Typical temporal signal recorded by a cluster of transducers.

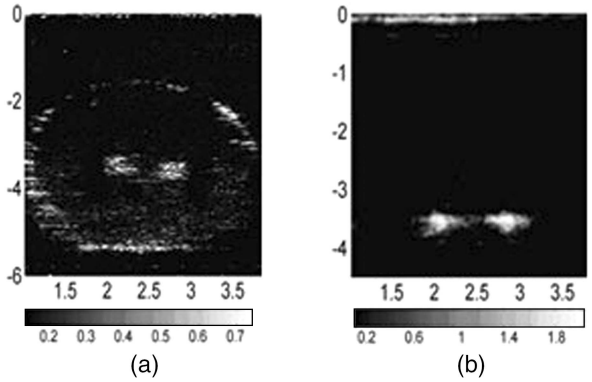

Fig. 3. (a) Ultrasound image of the phantom with embedded absorbers. The transducer is located on the top of the image (i.e., $y = 0$) and is parallel to the x axis. (b) Reconstructed PA image of the phantom with its embedded absorbers.

Electronically scanning dynamic clusters along the linear array allowed the corresponding ultrasound echoes and PA signals to be projected along the axis of the focusing zone. The reconstructed conventional ultrasonic image of the sample is shown in Fig. 3(a). The outline of the sample and the positions of the absorbers in the image are identifiable. The additional highlighted areas in the ultrasonic image are likely the result of gas bubbles or gelatin that was not completely dissolved.

In the PA tomograph reconstruction, PA signals were first deconvoluted with the impulse of the transducers, according to Eq. (2). The processed signals were projected with Eq. (1) to form a two-dimensional tomograph. Figure 3(b) is a reconstructed image of the absorbers. There was little indication of the phantom boundary, likely because of the low optical absorption of the materials used in the experiment, yet an object was observed at the position of the linear transducer array, which is likely due to the scattered laser light irradiating on the surface of the detectors. This was confirmed by the observation of signal D in Fig. 2. The experimental results confirmed what was predicted with our numerical simulation. Compared with those images based on the filter backprojection algorithm, there were fewer reconstruction artifacts when the PA signal was collected and processed with the algorithm similar to that for ultrasound image reconstruction.

In conclusion, we have developed an ultrasound and PA combination imaging system with a linear transducer array. The apparatus used conventional ultrasound to rapidly screen and locate potential targets. After a potential target is identified, the system can acquire the corresponding ultrasound and PA images simultaneously. With the system a PA signal is collected and processed by a phase-controlled focusing technique. This effectively reduces the artifacts in the condition of linear scanning. The corresponding ultrasound impedance and optical absorption images are likely to provide richer information for a better understanding of the target and subsequent diagnosis.

This research was supported by the National Major Fundamental Research Project of China (2002CCC00400), the National Natural Science Foundation of China (60378043), and the Research Team Project of the Natural Science Foundation of Guangdong Province (015012). D. Xing's e-mail address is xingda@scnu.edu.cn.

References

1. A. A. Oraevsky, S. L. Jacques, R. O. Esenaliev, and F. K. Tittel, Proc. SPIE **2134A,** 122 (1994).
2. G. A. Hoelen, F. F. M. de Mul, R. G. M. Kolkman, and A. Dekker, Opt. Lett. **23,** 648 (1998).
3. J. J. Niederhauser, D. Frauchiger, H. P. Weber, and M. Frenz, Appl. Phys. Lett. **81,** 571 (2002).
4. K. P. Köstli and P. C. Beard, Appl. Opt. **42,** 1899 (2003).
5. X. D. Wang, Y. J. Pang, G. Ku, X. Y. Xie, G. Stoica, and L. V. Wang, Nat. Biotechnol. **21,** 803 (2003).
6. Y. Yao, D. Xing, K. Ueda, and Q. Chen, J. Appl. Phys. **94,** 1278 (2003).
7. R. A. Kruger, W. L. Kiser, D. R. Reinecke, and G. A. Kruger, Med. Phys. **30,** 856 (2003).
8. A. A. Oraevsky, A. A. Karabutov, and S. V. Solomatin, Proc. SPIE **4256,** 6 (2001).
9. B. Zh. Yin, D. Xing, Y. Wang, Y. G. Zeng, Y. Tan, and Q. Chen, Phys. Med. Biol. **49,** 1339 (2004).
10. R. A. Kruger and L. P. Fang, Med. Phys. **22,** 1605 (1995).
11. J. Bai, *The Principle of Diagnostic Ultrasound Imaging* (Tsinghua U. Press, Beijing, 1998).
12. K. Larin, O. Hartrump, I. Larina, and R. Esenaliev, Proc. SPIE **4256,** 147 (2001).